frontiers | Frontiers in Sustainable Food Systems

TYPE Original Research
PUBLISHED 04 February 2026
DOI 10.3389/fsufs.2026.1765381

OPEN ACCESS

EDITED BY
Sujosh Nandi,
Swedish University of Agricultural Sciences, Sweden

REVIEWED BY
Soubhagya Tripathy,
Indian Institute of Technology Kharagpur, India
Tej Bhan Singh,
University of Petroleum and Energy Studies, India

*CORRESPONDENCE
Yuming Guo
✉ guoyuming99@sina.com

RECEIVED 11 December 2025
REVISED 11 January 2026
ACCEPTED 16 January 2026
PUBLISHED 04 February 2026

CITATION
Sun J, Qiu S, Feng H, Guo Y and Xu B (2026) Experimental determination of the mechanical properties of highland barley grains. *Front. Sustain. Food Syst.* 10:1765381. doi: 10.3389/fsufs.2026.1765381

Experimental determination of the mechanical properties of highland barley grains

Jingxin Sun[1], Shujin Qiu[2], Huimin Feng[1], Yuming Guo[2]* and Baohui Xu[1]

[1]Department of Mechanical and Electrical Engineering, Yuncheng University, Yuncheng, China, [2]College of Agricultural Engineering, Shanxi Agricultural University, Taiyuan, China

Background: The aim of this study was to investigate the conventional and viscoelastic mechanical properties of highland barley grains to provide a foundation for optimizing harvesting and processing equipment.

Methods: The triaxial dimensions, 1,000-grain weight, and unit weight of three highland barley varieties (Beiqing-7, Kunlun-5, and Yunqing-8) were determined at different moisture contents (9.0–22.9%). The friction coefficients and angles of repose of the grains were measured using an inclined plane instrument and an angle-of-repose measuring device. Stress relaxation and creep tests were conducted using a dynamic thermomechanical analyzer (Q800). The stress relaxation and creep data were fitted and analyzed using the Maxwell and Burgers models, respectively. The shear mechanical properties of the grains were measured using a texture analyzer.

Results: As the moisture content increased, the length, width, height, 1,000-grain weight, arithmetic mean diameter, and geometric mean diameter of the grains increased significantly, whereas the unit weight decreased. Moreover, the highest friction coefficient was observed between the grains and a Q235 steel plate. The friction coefficient and angle of repose decreased as the moisture content decreased. Furthermore, the shear failure force and shear failure stress of the grains increased gradually as the moisture content decreased. The Burgers model accurately described the creep behavior of the grains, whereas the three-element Maxwell model described their stress relaxation behavior. The model results indicated that increasing moisture content led to a decrease in elastic modulus and an increase in creep deformation. The triaxial dimensions, 1,000-grain weight, and unit weight of Beiqing-7 grains were the largest, and their mechanical properties were the most favorable. The friction coefficient of Yunqing-8 grains was the largest; however, their angle of repose was the smallest.

Conclusion: The findings of this study provide a scientific basis for the development of mechanized harvesting and processing equipment (peeling, flour milling, and storage) and for parameter optimization in highland barley production.

KEYWORDS

dynamic viscoelastic properties, frictional properties, highland barley grain, physical properties, shear properties

1 Introduction

Highland barley (*Hordeum vulgare* L. *var. nudum* Hook. f.) belongs to the family Poaceae (Sun et al., 2024; Zha and Wang, 2023) and is also referred to as naked barley or qingke barley (Wang et al., 2023). The crop is widely cultivated in China and is primarily grown in the Tibetan Plateau region, including Tibet, Qinghai Province (Aba), Ganzi in Sichuan Province, Diqing in Yunnan Province, and Gannan in Gansu Province (Zhang et al., 2025).

Highland barley is a coarse-grained crop, and the total investment in scientific research on the crop is relatively low. Mechanized harvesting of barley has accelerated in recent years (Jin, 2024), with only a few specialized harvesters being developed (Wang, 2023). Therefore, establishing physical parameters, including shear, friction, angle of repose, viscoelasticity, and other mechanical properties of highland barley, is necessary for developing the key components of highland barley segmentation and combined harvesting machinery (Dai et al., 2021), processing machinery, and highland barley uniform sowing machinery (Ding, 2022).

Experimental studies on the physical and mechanical properties of coarse grains, such as highland barley, millet, oats, and buckwheat, have been conducted. For example, Liu (2020) and Jin (2024) measured the triaxial size of highland barley grains using Vernier calipers. Sologubik et al. (2013) investigated the influence of moisture content on the physical properties of barley grains, such as length, width, height, arithmetic mean diameter, geometric mean diameter, 1,000-grain weight, coefficients of static friction, and angle of repose. The study concluded that moisture content had a substantial impact on the aforementioned physical properties, and a correlation was obtained through fitting. Zhu et al. (2017) investigated the influence of moisture content on the physical and viscoelastic properties of barley grains and concluded that moisture content is linearly related to the length, width, height, 1,000-grain weight, and grain volume. They also described the creep behavior of grains using the four-element Burgers model. Furthermore, Ding (2022) and Ding et al. (2021) measured the maximum static friction coefficient and angle of repose of highland barley grains using the inclined plane and cylinder lifting methods, respectively. Qiu et al. (2021) conducted shear tests on bare oat grains and concluded that moisture content and shear direction markedly affected the maximum shearing force of the grains, whereas the shear speed had no notable effect. Yang et al. (2015) investigated the compression and friction mechanical properties of millet grains. Sun et al. (2018) evaluated the compression, impact, and friction characteristics of buckwheat grains and the dynamic viscoelasticity of buckwheat flour. Cheng and Sun (2009) assessed the correlation between shear resistance and the quality of different wheat varieties and found pronounced differences in shear resistance among the varieties. Compared with the grains of wheat (He et al., 2025), rice (Duan et al., 2023), millet (Yang et al., 2015), and buckwheat (Sun et al., 2018), the grains of highland barley have a larger length–width ratio, and this indicator is a key physical parameter for the design optimization of cleaning devices (Jin, 2024). Moreover, considerable differences exist between the physical properties of different barley varieties (Liang et al., 2022). At present, relatively few studies have investigated the effects of variety on mechanical properties, such as shear, friction, angle of repose, and viscoelasticity, of highland barley grains. Therefore, this study systematically investigated the effects of variety and moisture content on physical parameters and mechanical properties, such as shear strength, friction characteristics, angle of repose, and viscoelasticity. These results provide a basis for simulation analysis and structural optimization of highland barley harvesting, sowing, and other related machinery. Furthermore, the experimental methods used in this study can serve as a reference for investigating the physical and mechanical properties of other grains and small granular particles.

2 Materials and methods

2.1 Materials

The following highland barley varieties were investigated: Beiqing-7 (from Xining City, Qinghai Province, China, east longitude: 101°33′, north latitude: 36°24′34″, altitude: 2,800 m), Kunlun-15 (from Hainan Tibetan Autonomous Prefecture, Qinghai Province, China, east longitude: 100°22′, north latitude: 36°09′, altitude: 2,940 m), and Yunqing-8 (from Diqing Tibetan Autonomous Prefecture, Yunnan Province, China, east longitude: 99°44′, north latitude: 27°54′, altitude: 3,270 m). The initial moisture content was determined using the drying method (Sologubik et al., 2013) with electric heating at a constant temperature in a blast-drying oven (DHG-9070A, Shanghai Yiheng Scientific Instrument Co., Ltd.). The initial moisture contents, measured using an electronic balance (Quintix224-1CN, Sartorius Scientific Instruments Beijing Co., Ltd., laboratory), were 22.90, 19.5, and 12.1%, respectively (wet basis; same below). The moisture content of highland barley at harvest is 16.8–22.9% (Liu, 2020), the safe moisture content of highland barley storage is below 13% (Zhu K. et al., 2023), the moisture content at sowing is approximately 9.0% (Ding, 2022), and the moisture content at wheat harvest is generally 17–25% (Ouyang et al., 2024; Wei, 2016). Therefore, the moisture contents of the samples were 9.0, 12.1, 16.4, 19.5, and 22.9%.

2.2 Instruments and equipment

An electrothermal constant-temperature blast-drying oven (Shanghai Yiheng Scientific Instrument Co., Ltd., DHG-9070A) was used to measure moisture content. An SU 5000 scanning electron microscope (Hitachi Company, Japan) and a high-definition camera stereo microscope (T2-HD228S, Shenzhen Aos Micro-Optical Instrument Co., Ltd.) were used to observe the microstructure of the highland barley grains and to take images. A digital Vernier caliper (accuracy: 0.01 mm) was used to measure the triaxial grain size. An electronic balance was used to measure the mass of the grain samples during moisture content determination. The specifications for Quintix 224-1 CN (Sartorius Scientific Instruments Beijing Co., Ltd.) were as follows: the actual indexing value was 0.1 mg, and the maximum weight was 220 g. The specifications for BSA3202S-CW (Sartorius Scientific Instruments Beijing Co., Ltd.) were as follows: the actual indexing value

was 0.01 g, and the maximum weight was 3,200 g. A *TA.XT* texture analyzer was used to measure parameters during shear experiments (Stable Micro Systems, UK). The distance resolution was 0.001 mm, and the test speed ranged from 0.01 to 40 mm·s^{-1}. Samples were stored in a medical freezer (YCD-FL289; Zhongke Meiling Cryogenic Technology Co., Ltd., China). A TR211 surface roughness instrument (Beijing Time Ryda Technology Co., Ltd., China), with a measurement accuracy of 1×10^{-6} mm, was used to measure surface roughness. A dynamic thermomechanical analyzer (DMA Q800) was used for the stress relaxation and creep experiments of highland barley grains (TA Instruments, USA; modulus accuracy ±1%). Moreover, a self-made inclinometer and angle-of-repose measuring device were used. An automatic ion sputtering instrument (108 AUTO, TED PELLA, INC), a digital Vernier caliper (JDF01, Dongguan Sanliang Precision Measuring Instrument Co., Ltd., China, accuracy 0.01 mm), and a digital angle ruler (JCD01, Dongguan Sanliang Precision Measuring Instrument Co., Ltd., China, accuracy 0.01°) were used.

2.3 Preparation of experimental samples

Five initial moisture content samples of the three varieties were accurately weighed using an electronic balance (BSA3202S-CW, Sartorius Scientific Instruments Beijing Co., Ltd. laboratory), each of which weighed 1,000 g. The samples were placed in a well-sealed dry dish. Samples with a required moisture content higher than the initial moisture content were evenly sprayed with deionized water several times and stirred during spraying. The samples were stirred every 3–4 h. After 24 h, the prepared samples were placed in double-layer sealed plastic bags (340 mm × 240 mm) and stored in a refrigerator (YCD-FL289, Zhongke Meiling Cryogenic Technology Co., Ltd.) at 1 ± 0.5 °C for 3 days. During this period, the samples were shaken 3–5 times per day to ensure uniform water absorption (Yang et al., 2015). The mass of deionized water added was calculated using Equation 1:

$$m_1 = m_0 \frac{(\omega_1 - \omega_0)}{(1 - \omega_1)} \tag{1}$$

where ω_0 and ω_1 (%) are the initial moisture content of the samples and the required moisture content on a wet basis, respectively; and m_0 and m_1 (g) are the initial mass of highland barley and the mass of deionized water, respectively.

For highland barley with a required moisture content lower than the initial moisture content, single-layer grains were placed in a 600-mm-long and 400-mm-wide stainless steel tray for natural drying. The tray was placed indoors to reduce the moisture content by evaporation (Sun et al., 2018). During this period, the mass was measured every hour, and the moisture mass to be evaporated was calculated using Equation 1. When the reduced moisture mass equaled the required evaporation mass, the moisture content was determined using the drying method. The prepared samples were loaded into double-layer sealed plastic bags (340 mm × 240 mm) and stored at 1 ± 0.5 °C.

Before each experiment, the samples were equilibrated at room temperature (22 ± 2 °C) for 0.5 h.

2.4 Measurement of basic physical parameters of highland barley grain

Samples with different moisture content were prepared according to the methods described by Sun et al. (2018). The 1,000-grain mass was measured using the 100-grain method. Briefly, 100 random, undamaged, and pest-free grains were measured using an electronic balance (Quintix224-1CN, Sartorius Scientific Instruments Beijing Co., Ltd., laboratory) and multiplied by 10 to obtain the 1,000-grain weight (Sologubik et al., 2013). Each sample was analyzed three times. The length, width, and height of the grain were measured using a digital Vernier caliper (JDF01, Dongguan Sanliang Precision Measuring Instrument Co., Ltd.) (Sologubik et al., 2013) (30 grains per sample). The arithmetic mean diameter (D_a), geometric mean diameter (D_g), and sphericity (%) of the grains were calculated as follows:

$$D_a = \frac{(L + W + H)}{3} \tag{2}$$

$$D_g = (L \cdot W \cdot H)^{\frac{1}{3}} \tag{3}$$

$$S_P = \frac{(L \cdot W \cdot H)^{\frac{1}{3}}}{L} \times 100\% \tag{4}$$

where D_a, D_g, L, W, and H are the arithmetic mean diameter, geometric mean diameter, length, width, and height of the grain, respectively (mm). S_P represents the sphericity.

The unit weight was measured using the measuring cylinder method (Li et al., 2022). The sample was poured into a 1,000-mL measuring cylinder. The grains exceeding the upper limit of the scale of the measuring cylinder were scraped off with a ruler, and the mass was weighed using an electronic balance (BSA3202S-CW, Sartorius Scientific Instruments Beijing Co., Ltd., laboratory). The unit weight is the ratio of the mass of the grains in the measuring cylinder to the volume of the measuring cylinder (Li et al., 2022).

A blade was used to cut the grains along the ventral groove to observe their internal structure clearly. The treated samples were placed in a stereomicroscope (T2-HD228S, Shenzhen Aos Micro-Optical Instrument Co., Ltd., laboratory), and the magnification was gradually adjusted until the grains were magnified 18×. A complete longitudinal section of the grain was clearly observed, and a microscopic photograph was taken to obtain Figure 1c. The middle position was cross-cut along the grain length direction, and the same observation and photography method was used to increase the magnification to 25× to obtain Figure 1e.

The samples were cut longitudinally and transversely along the ventral groove of the grain and the middle part of the grain length. The treated samples were bonded to a metal round table with double-sided conductive adhesive, and the surfaces of the samples were plated using an automatic ion sputtering instrument (108AUTO, TED PELLA, INC). A thin layer of gold film was then applied, and the samples were observed using a scanning electron microscope (SU5000, Hitachi Company, Japan). The round metal table was magnified 14× and 25× at an acceleration voltage of 15 kV to obtain Figures 1d, f.

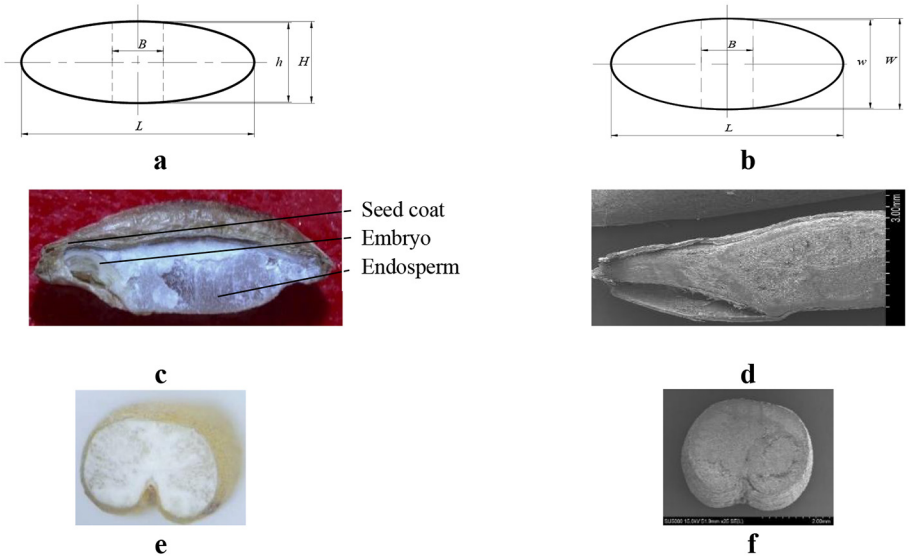

FIGURE 1
Triaxial size and the longitudinal and cross-sections of highland barley grain. **(a)** Main view of highland barley grain (length and height). **(b)** Top view of highland barley grain (width). **(c)** Longitudinal section of grain under a microscope (×18 magnification). **(d)** Longitudinal section of grain under a scanning electron microscope (×14 magnification). **(e)** Cross-section of grain under a microscope (×25 magnification). **(f)** Cross-section of grain under a scanning electron microscope (×25 magnification).

2.4.1 Friction coefficient and angle-of-repose measurements

The single-layer grain was placed in a bottomless container (40 mm length, 40 mm width, and 10 mm height) and placed on a slope meter (Sologubik et al., 2013) so that the inclination angle gradually increased. When a grain slides on a slope, the inclination angle of the slope corresponds to the static sliding friction angle. The slope meter directly read the angle using a digital angle ruler (JCD01, Dongguan Sanliang Precision Measuring Instrument Co., Ltd.) (Sun et al., 2018). The self-made instrument and the force diagram are shown in Figures 2a, b, respectively.

Equation 5 can be obtained from the force analysis in Figure 2b.

$$\mu = tan\alpha \tag{5}$$

where α is the angle (°) between the inclined plane and the horizontal plane, and μ is the friction coefficient (Sun et al., 2018).

The angle of repose reflects the internal friction and scattering performance of the grain group. The angles of repose of the grains were determined using the injection method (Sun et al., 2018). The measurement device is illustrated in Figure 3. The volume of the funnel was 0.4 L, the distance between the funnel outlet and the upper surface of the block was 40 mm, and the diameter of the block was 88 mm. During the experiment, 200 g of grains were loaded into the funnel, and the funnel outlet was opened, so that the grains fell naturally and continuously onto the upper surface of the cushion block. The angle between the cone generatrix accumulated by the grains and the ground plane is the angle of repose (Yang et al., 2016). The accumulation height (h) was measured, and the angle of repose was calculated according to Equation 6.

$$\varphi = arctg\left(\frac{2h}{D}\right) \tag{6}$$

where ϕ is the angle of repose (°); h is the height of the grain cone (mm); and D is the diameter of the base block (mm) (Sun et al., 2018).

Surface roughness was measured using a surface roughness instrument (TR211, Beijing Time Ryda Technology Co., Ltd., China, laboratory). The measured surface was cleaned before each experiment, and the instrument was placed horizontally on the measured surface to ensure that the sliding trajectory of the sensor was perpendicular to the processing texture direction of the measured surface. During measurement, the sensor slid approximately 5 mm at a speed of 1 mm·s^{-1} on the measured surface to obtain the surface roughness value.

2.4.2 Calculation of shear mechanical properties

The compression mode of the experimental texture analyzer (TA.XT plus, Stable Micro Systems, UK, laboratory) was selected, and a self-made double-sided shear blade and shear fixture were used as the shear device. The shear blade thickness was 2 mm. The shearing device is shown in Figure 4.

The parameters were set as follows: the pre-experiment speed was 0.5 mm·s^{-1}, the experiment speed was 0.01 mm·s^{-1}, the post-experiment speed was 1.0 mm·s^{-1}, the trigger force was 0.049 N, and the instrument was preheated for 20 min in advance. Before each experiment, the triaxial size of the highland barley grains was measured using a digital display Vernier caliper. The measured grain was placed vertically in the middle of the shear port such that the middle of the grain was sheared. The shear position is shown as a dashed line in Figures 1a, b.

The main and top views of the highland barley grain were approximately considered ellipses. The main and top views are shown in Figures 1a, b, respectively.

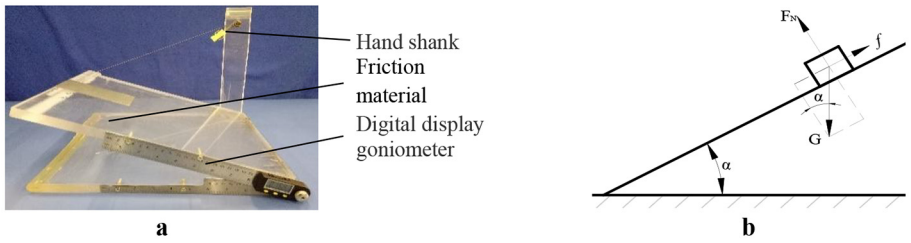

FIGURE 2
Bevel instrument and schematic diagram of force. **(a)** Bevel instrument. **(b)** Schematic diagram of force. *G*, *f*, and F_N are the gravity, friction, and support of the grain, respectively; and α is the angle between the inclined and horizontal planes.

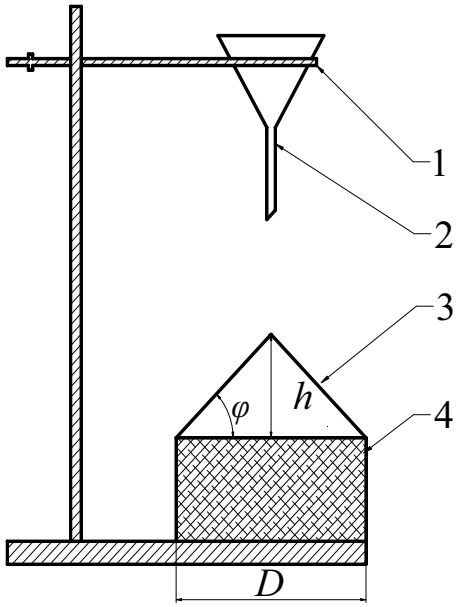

FIGURE 3
Angle-of-repose measurement device. 1: iron support, 2: funnel, 3: grain windrow, 4: block.

The elliptic equation obtained from Figure 1a is as follows:

$$\frac{x^2}{a^2}+\frac{z^2}{c^2}=1 \tag{7}$$

When $x = B/2$,

$$c' = z = \frac{c}{a}\sqrt{a^2-\frac{B^2}{4}} \tag{8}$$

The elliptic equation obtained from Figure 1b is as follows:

$$\frac{x^2}{a^2}+\frac{y^2}{b^2}=1 \tag{9}$$

When $x = B/2$,

$$b' = y = \frac{b}{a}\sqrt{a^2-\frac{B^2}{4}} \tag{10}$$

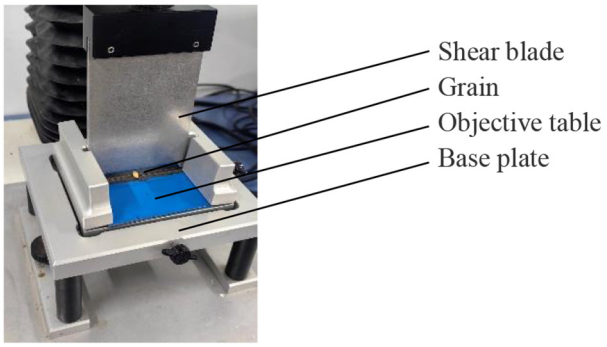

FIGURE 4
Shearing device of the texture analyzer.

The shear surface area is as follows:

$$A_s = \pi b' c' \tag{11}$$

Substituting $L = 2a$, $W = 2b$, $H = 2c$, $w = 2b\prime$, and $h = 2c\prime$ into Equation 8 generates the following equation:

$$A_s = \frac{\pi hw}{4} = \frac{\pi HW}{L^2}\left(\frac{L^2}{4}-\frac{B^2}{4}\right) \tag{12}$$

Hence, the shear failure stress is calculated as follows:

$$\tau_s = \frac{F_s}{2A_s} = \frac{2F_s \cdot L^2}{\pi HW\left(L^2-B^2\right)} \tag{13}$$

In Equations 7–13, B is the thickness (mm) of the shear blade (2 mm); A_s is the area of the shear plane (mm^2); F_s is the shear failure force (N); τ_s is the shear failure stress ($N{\cdot}mm^{-2}$); and b' and c' (mm) are the lengths of the long and short half axes of the shear position, respectively.

2.4.3 Calculation of viscoelastic properties

Highland barley grains are viscoelastic (Qiu et al., 2019). Thus, when analyzing the linear viscoelasticity of grains, assessing their stress relaxation and creep properties is also necessary (Ma, 2015). A dynamic thermal mechanical analyzer (DMA, TA Company,

USA) is an ideal instrument for determining the viscoelastic properties of highland barley grains (Chen et al., 2019).

Generally, the viscoelastic properties of grains are determined by evaluating their stress relaxation and creep properties. Creep refers to the process of applying a load to the linear viscoelastic region of a viscoelastic material to deform and keep the load unchanged while monitoring strain changes with time. Stress relaxation refers to the process in which a load is applied to the linear viscoelastic region of a viscoelastic body to cause a certain deformation, keep the deformation unchanged, and monitor the stress changes with time.

Highland barley is a viscoelastic material. Hence, a single elastomer, viscous, or plastic material cannot express the properties of grains (Ma, 2015). Therefore, to investigate the viscoelastic properties of grains, establishing a mechanical model suitable for complex viscoelastic materials is necessary. Common mechanical models include the Hooke, damping, Maxwell, and four-element models, which are also known as the Burgers model (Li et al., 2025), as shown in Figures 5a–d, respectively.

The Hooke and damping models, also called basic elements, are simple models. The Maxwell model is composed of a Hooke model and a damping model in series. The Kelvin–Voigt model is composed of a Hooke model and a damping model in parallel. This model is the most commonly used mechanical model for studying the viscoelastic properties of viscoelastic materials. The Burgers model, which is also known as the four-element model, is composed of the Maxwell and Kelvin–Voigt models in series. Generally, the Burgers model better describes the viscous and elastic deformations of a viscoelastic material under an external load. The Burgers model is represented by Equation 14.

$$\varepsilon(t) = \frac{\sigma}{E_0} + \frac{\sigma}{E_r}\left[1 - \exp\left(-\frac{t}{\tau_r}\right)\right] + \frac{\sigma}{\eta}t \tag{14}$$

where $\varepsilon(t)$ represents the strain (%) of the highland barley sample at time t; σ represents the constant stress ($N{\cdot}mm^{-2}$); E_0 and $E_r$represent the instantaneous and delayed elastic moduli ($N{\cdot}mm^{-2}$), respectively; τ_r represents the lag time (s); and η is the viscosity coefficient ($N{\cdot}s{\cdot}mm^{-2}$).

The three-element Maxwell model is represented by Equation 15.

$$\sigma(t) = E_1 exp\left(-\frac{t}{\tau_1}\right) + E_c \tag{15}$$

where $\sigma(t)$ represents the stress ($N{\cdot}mm^{-2}$) of the highland barley sample at time t; E_1 and E_c represent the decay elastic modulus ($N{\cdot}mm^{-2}$) and equilibrium elastic modulus ($N{\cdot}mm^{-2}$), respectively; and τ_1 is the relaxation time (s).

The creep experiment on highland barley grains was conducted using the compression fixture of the DMA Q800 instrument, and the stress was set as 0.02 $N{\cdot}mm^{-2}$. The creep experimental procedure was as follows:

(1) Data storage off.
(2) Equilibrate at 25.00 °C.
(3) Isothermal for 2 min.
(4) Data storage on.
(5) Displace 5.00 min recover 5.00 min.
(6) Repeat segment 5 for 2 times.

The strain was set to 0.8, and the stress relaxation experiment procedure was as follows:

(1) Data storage off.
(2) Equilibrate at 25.00 °C.
(3) Isothermal for 2 min.
(4) Data storage on.
(5) Displace 10.00 min recover 0 min.

Before each stress relaxation and creep experiment, the two ends (along the length direction) of the grain were ground slightly using metallographic sandpaper, and the upper and lower ends of the grain were ground into a plane. The ground highland barley sample was regarded as a cylinder with two elliptical cross sections. The experiment program selected in the DMA Q800 instrument was "a cylinder with a round bottom." Therefore, an equivalent diameter was required. The equation for the equivalent diameter is expressed in Equation 16.

$$d = \sqrt{W \cdot H} \tag{16}$$

where d represents the equivalent diameter (mm) of the sample.

Before the experiment, the DMA Q800 instrument was preheated for more than 30 min, and "position calibration" and "fixture calibration" were carried out sequentially after starting the instrument. Stress relaxation and creep experiments on highland barley grains were conducted using the DMA compression mode, and the preload force was 0.01 N.

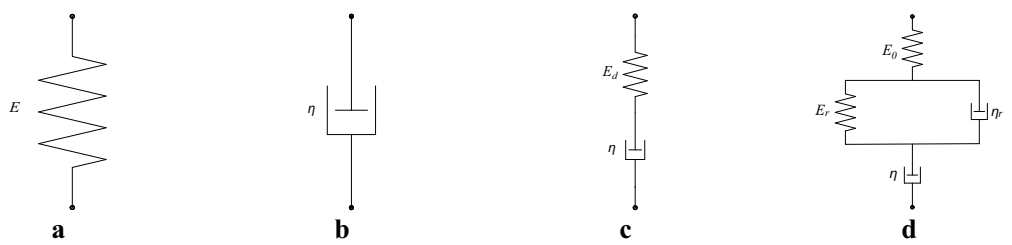

FIGURE 5
Basic mechanical models of viscoelasticity. **(a)** Hooke model. **(b)** Damping model. **(c)** Maxwell model. **(d)** Burgers model.

2.5 Data processing

The data were processed using Microsoft Excel v2019. Figures were produced using Origin v2018, which is a scientific drawing and data analysis software developed by OriginLab that can run under Microsoft Windows. Statistical significance was determined using analysis of variance, generalized linear models, and other procedures in SAS v8 (Statistical Analysis System) statistical software. The regression models were produced using MATLAB v2016 (business mathematics software developed by MathWorks, USA).

3 Results

3.1 Basic parameters of highland barley grains

The basic physical parameters and statistical analysis results of highland barley grains under different moisture contents are shown in Tables 1, 2.

As shown in Table 2, variety and moisture content had significant effects on the length, width, height, unit weight, arithmetic mean diameter, geometric mean diameter, sphericity, and 1,000-grain weight of highland barley grains ($P < 0.05$).

As shown in Table 1, when the moisture content increased from 9.0% to 22.9%, the length, width, height, 1,000-grain weight, arithmetic mean diameter, geometric mean diameter, and sphericity of the grains increased, whereas the unit weight decreased as the moisture content increased. The increase in grain size was attributed to the expansion of the grain surface, internal coarse capillaries, and intercellular spaces caused by water absorption. As the moisture content increases, the degree of transverse expansion of grains is markedly greater than that of the longitudinal expansion (Song, 2019); thus, the sphericity also gradually increases. Grains of the three highland barley varieties exhibited similar changes, and similar trends have been reported for wheat (Liu, 2023; Chen, 2025) and barley (Sologubik et al., 2013; Carvalho et al., 2021). The length, width, height, arithmetic mean diameter, geometric mean diameter, 1,000-grain weight, and unit weight of Beiqing-7 were the highest, whereas those of Yunqing-8 were the lowest.

TABLE 1 Basic physical parameters of highland barley grains.

Variety name	Moisture content/%	Length/mm	Width/mm	Height/mm	1,000-grain weight/g	Unit weight/(g·L-1)	Arithmetic mean diameter/mm	Geometric mean diameter/mm	Sphericity
Beiqing-7	22.9	8.85 ± 0.52a	3.86 ± 0.21a	2.84 ± 0.19a	53.21 ± 0.57a	672.54 ± 2.19e	5.18 ± 0.22a	4.59 ± 0.20a	51.92 ± 2.50a
	19.5	8.74 ± 0.51b	3.78 ± 0.18b	2.78 ± 0.15b	51.78 ± 0.51b	682.54 ± 2.29d	5.10 ± 0.21ab	4.51 ± 0.17a	51.65 ± 2.09b
	16.4	8.60 ± 0.38c	3.72 ± 0.22c	2.72 ± 0.17c	50.34 ± 1.57c	734.05 ± 1.74c	4.98 ± 0.21bc	4.38 ± 0.22b	50.91 ± 2.25c
	12.1	8.39 ± 0.42cd	3.67 ± 0.29d	2.66 ± 0.18d	47.09 ± 0.71d	755.23 ± 3.80b	4.91 ± 0.18c	4.34 ± 0.19b	50.80 ± 3.05d
	9.0	8.25 ± 0.48e	3.63 ± 0.27e	2.62 ± 0.16e	44.72 ± 0.82e	767.67 ± 6.26a	4.84 ± 0.21c	4.28 ± 0.20b	50.00 ± 3.10e
Kunlun-5	22.9	8.54 ± 0.54a	3.84 ± 0.23a	2.83 ± 0.31a	48.95 ± 0.07a	653.80 ± 1.91e	5.06 ± 0.14a	4.52 ± 0.13a	53.07 ± 1.26a
	19.5	8.36 ± 0.42b	3.76 ± 0.17b	2.72 ± 0.17b	46.33 ± 0.38b	675.01 ± 3.81d	4.94 ± 0.25b	4.41 ± 0.23b	52.70 ± 1.19b
	16.4	8.25 ± 0.42c	3.72 ± 0.16c	2.67 ± 0.16c	45.08 ± 0.17c	716.91 ± 2.31c	4.88 ± 0.24c	4.34 ± 0.22c	52.65 ± 2.19c
	12.1	8.12 ± 0.46d	3.66 ± 0.17d	2.62 ± 0.17d	42.98 ± 0.85d	742.45 ± 4.79b	4.80 ± 0.26d	4.27 ± 0.23d	52.61 ± 1.92d
	9.0	7.88 ± 0.36e	3.56 ± 0.25e	2.54 ± 0.24e	40.24 ± 0.49e	758.07 ± 1.67a	4.66 ± 0.18e	4.15 ± 0.17e	52.59 ± 1.97e
Yunqing-8	22.9	8.53 ± 0.46a	3.83 ± 0.13a	2.73 ± 0.20a	48.14 ± 0.17a	646.73 ± 4.12e	5.03 ± 0.18a	4.48 ± 0.14a	55.49 ± 3.46a
	19.5	8.34 ± 0.52b	3.73 ± 0.23b	2.67 ± 0.14b	45.87 ± 0.50b	661.60 ± 1.43d	4.91 ± 0.29b	4.36 ± 0.26b	53.84 ± 2.46b
	16.4	8.18 ± 0.49c	3.66 ± 0.22c	2.63 ± 0.14c	44.07 ± 0.27c	702.63 ± 1.30c	4.82 ± 0.28c	4.28 ± 0.24c	52.61 ± 2.59c
	12.1	8.05 ± 0.51d	3.59 ± 0.23d	2.58 ± 0.14d	42.20 ± 0.13d	724.37 ± 2.11b	4.74 ± 0.29d	4.21 ± 0.25d	50.97 ± 2.03d
	9.0	7.84 ± 0.35e	3.49 ± 0.31e	2.49 ± 0.24e	39.33 ± 0.29e	745.63 ± 3.19a	4.61 ± 0.20e	4.08 ± 0.16e	49.23 ± 2.90e

The values in the table are reported as the mean ± standard deviation. Different lowercase letters in the same column indicate significant differences ($P < 0.05$) among the treatments. This notation is consistent with Tables 4, 6.

TABLE 2 Statistical analysis of basic physical parameters of highland barley grains (*P*-values).

Source of variation	Length/mm	Width/mm	Height/mm	1,000-grain weight/g	Unit weight/(g·L-1)	Arithmetic mean diameter/mm	Geometric mean diameter/mm	Sphericity	Angle of repose/(°)
Variety	< 0.0001	0.00402	< 0.0001	< 0.0001	< 0.0001	< 0.0001	< 0.0001	< 0.0001	< 0.0001
Moisture content	< 0.0001	< 0.0001	< 0.0001	< 0.0001	< 0.0001	< 0.0001	< 0.0001	< 0.0001	< 0.0001

3.2 Shear properties of highland barley grains

As shown in Table 3, the effects of variety and moisture content on the shear failure force, deformation quantity, shear failure energy, and shear failure stress of highland barley grains were extremely significant ($P < 0.0001$). The coefficients of determination (R^2) were 0.87, 0.77, 0.82, and 0.88, respectively. According to the *F*-value, the main factors affecting the mechanical properties of highland barley grains were moisture content and variety. As shown in Table 4, with a decrease in moisture content, the shear failure force and shear failure stress of highland barley grains gradually increased, whereas the shear failure energy initially decreased and then subsequently increased, and the deformation gradually decreased.

The lower the moisture content, the greater the grain hardness, shear failure force, and shear failure stress. With a decrease in moisture content, the brittleness of grains increases, and toughness decreases (Zhu X. et al., 2023); hence, the deformation of shear failure decreases gradually. The variation patterns of the shear failure force and stress of highland barley grains with moisture content were consistent with those of bare oats (Qiu et al., 2021). The shear failure energy first decreases and then increases with a decrease in moisture content, which differs from the variation pattern of bare oats (Qiu et al., 2021). This was because the shear failure energy was related to both the shear failure force and deformation. When the moisture content was high, the grain hardness was low, the shear failure force was relatively low, and the shear failure energy was greatly affected by deformation, which is consistent with the variation pattern of deformation. When the moisture content was low, the grain hardness increased, the shear failure force rapidly increased, and the deformation change was relatively small. The shear failure energy was therefore mainly affected by the shear failure force, which is consistent with the variation pattern of the shear failure force.

The shear failure force, deformation, shear failure energy, and failure stress of the three varieties of highland barley differed, and those of Beiqing-7 were the highest. Taking Beiqing-7 as an example, the regression models of the shear mechanical property indices and moisture content were fitted using MATLAB v2016 (Table 5). As shown in Table 5, a linear relationship was found between the shear failure force, shear failure stress, and moisture content, whereas a quadratic polynomial relationship was found between the deformation quantity and moisture content. The R^2 values were greater than 0.9, indicating good fitting accuracy.

TABLE 3 Analysis of variance of the shear experiment results for highland barley grains.

Source of variation	Degree of freedom	Failure load of shear/N		Deformation quantity/mm		Failure energy of shear/(N·mm)		Shear failure stress/(N·mm^{-2})	
		F-value	*P*-value	*F*-value	*P*-value	*F*-value	*P*-value	*F*-value	*P*-value
Variety	2	14.40	<0.0001	7.09	0.0011	7.38	<0.0001	77.89	<0.0001
Moisture content	4	320.47	<0.0001	154.12	<0.0001	17.92	<0.0001	294.87	<0.0001

TABLE 4 Shear experiment results of highland barley grain.

Variety name	Moisture content/%	Shear failure force/N	Deformation quantity/mm	Shear failure energy/(N·mm)	Shear failure stress/(N·mm^{-2})
Beiqing-7	22.9	44.50 ± 6.32e	1.25 ± 0.24a	30.53 ± 7.74a	3.06 ± 0.52d
	19.5	55.51 ± 7.35d	0.96 ± 0.24b	20.34 ± 9.03c	3.34 ± 0.39d
	16.4	68.49 ± 10.44c	0.75 ± 0.09c	26.41 ± 6.36b	4.60 ± 0.53c
	12.1	90.63 ± 11.86b	0.64 ± 0.06cd	27.82 ± 5.15ab	6.12 ± 0.65b
	9.0	100.56 ± 10.75a	0.59 ± 0.06d	29.30 ± 5.00ab	6.84 ± 0.89a
Kunlun-5	22.9	41.90 ± 4.72e	1.15 ± 0.16a	28.50 ± 5.08a	2.63 ± 0.33e
	19.5	51.24 ± 4.07d	0.90 ± 0.13b	19.29 ± 2.40d	3.14 ± 0.24d
	16.4	64.61 ± 2.23c	0.73 ± 0.09c	23.32 ± 4.87c	4.14 ± 0.65c
	12.1	82.58 ± 2.68b	0.63 ± 0.04d	25.74 ± 6.63b	4.69 ± 0.19b
	9.0	94.51 ± 3.49a	0.54 ± 0.03e	27.59 ± 2.99a	5.06 ± 0.43a
Yunqing-8	22.9	38.95 ± 5.98e	1.08 ± 0.15a	27.77 ± 7.84a	2.59 ± 0.47e
	19.5	48.68 ± 6.2d	0.88 ± 0.08b	18.14 ± 5.50d	3.10 ± 0.36d
	16.4	60.15 ± 3.83c	0.71 ± 0.06c	21.07 ± 5.44c	3.59 ± 0.41c
	12.1	79.15 ± 4.25b	0.59 ± 0.07d	23.11 ± 4.71b	4.44 ± 0.60b
	9.0	89.44 ± 4.71a	0.52 ± 0.03e	25.97 ± 0.91a	4.66 ± 0.18a

Different lowercase letters indicate the significant difference in shear mechanical properties of the same variety for highland barley grains under different moisture contents ($P < 0.05$).

10.3389/fsufs.2026.1765381

3.3 Friction mechanical properties of highland barley grains

The results and statistical analysis of the friction coefficient and angle of repose of highland barley grains with different moisture contents are shown in Tables 6, 7, respectively.

Commonly used materials for harvesting, seeding, and processing machinery include stainless steel (Lu, 2024), 7075 aluminum alloy (Cui et al., 2016), and Q235 steel (Jin, 2024; Liu, 2020). The order of roughness of these three materials is as follows: stainless steel plate (Ra = 0.201 μm) < aluminum plate (Ra = 0.325 μm) < Q235 steel plate (Ra = 0.841 μm). Table 7 shows that variety, moisture content, and friction material had very significant effects on the friction coefficient ($P < 0.0001$). The coefficient of determination (R^2) for the model was 0.98. According to the F-value, the main factors affecting the friction coefficient of highland barley were moisture content, friction material, and variety. As shown in Table 6, the friction coefficient between highland barley grains and the Q235 steel plate was the largest, followed by the 7075 aluminum alloy plate, whereas the friction coefficient between grains and the stainless steel plate was the smallest. Thus, the larger the surface roughness of the material, the greater the friction resistance and friction coefficient. With an increase in the moisture content, the friction coefficients between the grains and the stainless steel, 7075 aluminum alloy, and Q235 steel plates increased gradually. The variation in friction coefficient with moisture content was consistent with that observed for buckwheat (Sun et al., 2018) and wheat (Jia et al., 2025). Furthermore, as the moisture content increased, the adhesion force between the grains and the contact material increased, leading to increased friction resistance, a higher friction coefficient, deteriorated fluidity, and a corresponding increase in the angle of repose. The three highland barley varieties exhibited similar trends. Under the same friction material and moisture content, the friction coefficient of Yunqing-8 was the largest, whereas that of Beiqing-7 was the smallest.

TABLE 5 Regression models of shear mechanical property indices, friction coefficient, angle of repose, and moisture content for highland barley grains.

Mechanical properties	Regression model	R^2
Shear mechanical properties	$F_s = -4.1975x + 139.01$	0.9935
	$\Delta = 0.0037x^2 - 0.0714x + 0.9419$	0.9974
	$\tau_s = -0.2948x + 9.5032$	0.9725
Friction mechanical properties	$\mu_s = 0.0077x + 0.2354$	0.9816
	$\mu_a = 0.0074x + 0.2691$	0.9979
	$\mu_i = 0.0069x + 0.2993$	0.999
	$\varphi = 0.4729x + 30.299$	0.9854

F_s, Δ, τ_s, and x represent shear failure force (N), deformation quantity (mm), shear failure stress (N·mm^{-2}), and moisture content. μ_s, μ_a, μ_i, and ϕ represent the friction coefficients for the 304 stainless steel plate, 7075 aluminum alloy plate, and Q235 steel plate, and the angle of repose, respectively. R^2 is the coefficient of determination.

TABLE 7 Analysis of variance of the friction coefficient of highland barley grains.

Source of variation	Degree of freedom	F-value	P-value
Variety	2	134.49	<0.0001
Moisture content	4	1,151.35	<0.0001
Friction material	2	748.76	<0.0001

TABLE 6 Friction coefficient and angle of repose of highland barley grains under different moisture contents.

Variety name	Moisture content/%	304 stainless steel plate	7075 aluminum alloy plate	Q235 steel plate	Angle of repose/(°)
Beiqing-7	22.9	0.411 ± 0.004a	0.436 ± 0.007a	0.457 ± 0.006a	41.40 ± 0.42a
	19.5	0.394 ± 0.008b	0.416 ± 0.006b	0.435 ± 0.007b	39.51 ± 0.26b
	16.4	0.354 ± 0.004c	0.391 ± 0.009c	0.415 ± 0.005c	37.51 ± 0.27c
	12.1	0.332 ± 0.003d	0.358 ± 0.011d	0.383 ± 0.007d	36.14 ± 0.25d
	9.0	0.305 ± 0.008e	0.335 ± 0.004e	0.361 ± 0.013e	34.72 ± 0.29e
Kunlun-5	22.9	0.428 ± 0.007a	0.447 ± 0.002a	0.471 ± 0.009a	39.03 ± 0.22a
	19.5	0.400 ± 0.006b	0.427 ± 0.003b	0.445 ± 0.006b	37.11 ± 0.26b
	16.4	0.361 ± 0.006c	0.402 ± 0.009c	0.425 ± 0.006c	35.49 ± 0.25c
	12.1	0.338 ± 0.002d	0.365 ± 0.004d	0.398 ± 0.007d	32.89 ± 0.35d
	9.0	0.313 ± 0.009e	0.341 ± 0.002e	0.365 ± 0.007e	31.85 ± 0.19e
Yunqing-8	22.9	0.438 ± 0.004a	0.461 ± 0.004a	0.482 ± 0.004a	37.79 ± 0.37a
	19.5	0.410 ± 0.004b	0.437 ± 0.006b	0.456 ± 0.007b	35.16 ± 0.27b
	16.4	0.378 ± 0.006c	0.416 ± 0.005c	0.436 ± 0.009c	33.79 ± 0.39c
	12.1	0.351 ± 0.004d	0.377 ± 0.004d	0.418 ± 0.003d	32.39 ± 0.10d
	9.0	0.321 ± 0.007e	0.355 ± 0.004e	0.376 ± 0.005e	30.91 ± 0.26e

Different small letters indicate that the friction coefficients between highland barley grains and different friction materials are significantly different at the 0.05 level.

As shown in Table 2, the moisture content had a significant effect on the angle of repose ($P < 0.0001$). As the moisture content increased, the angle of repose increased. The relationships between friction coefficient (for the same friction material), moisture content, and angle of repose of highland barley grains were approximately linear. The fitted regression models are presented in Table 5, and the R^2 values were greater than 0.98, indicating good fitting relationships.

3.4 Viscoelastic properties of highland barley grains

The creep and stress relaxation curves of highland barley grains with different moisture contents are shown in Figures 6, 7, respectively.

Under the same moisture content, the creep process included three stages (Figure 6). The first stage was instantaneous elastic deformation after applying a constant load to the highland barley grain sample. This deformation was reversible and expressed by the spring element in the Maxwell model. The second stage was the creep stage of the highland barley grain sample under constant stress. Deformation at this stage required a relaxation time and was expressed by the Kelvin–Voigt model (Li et al., 2025). The third stage was the recovery stage after unloading, which required a certain time for recovery and was expressed by the damper element of the Maxwell model. During the 300 s creep process, the strain of highland barley grains increased rapidly at first and then increased slowly with time. During the 300 s recovery process, the strain decreased with time. When the moisture content ranged from 9.0% to 22.9%, the strain values of the grains increased with increasing moisture content. This trend is consistent with that reported for maize kernels (Sheng, 2016). The creep curves of the three varieties were similar. Taking Beiqing-7 as an example, the Burgers model was used to fit the creep process of highland barley grains, and the regression models and corresponding P-values are shown in Table 8. The P-values of all regression models were less than 0.0001.

The instantaneous elastic modulus E_0 represents the instantaneous response described by the Hooke model and characterizes material elasticity (Li et al., 2025), whereas the delayed elastic modulus E_r characterizes material hardness. As shown in Table 8, with increasing moisture content, E_0 and E_r

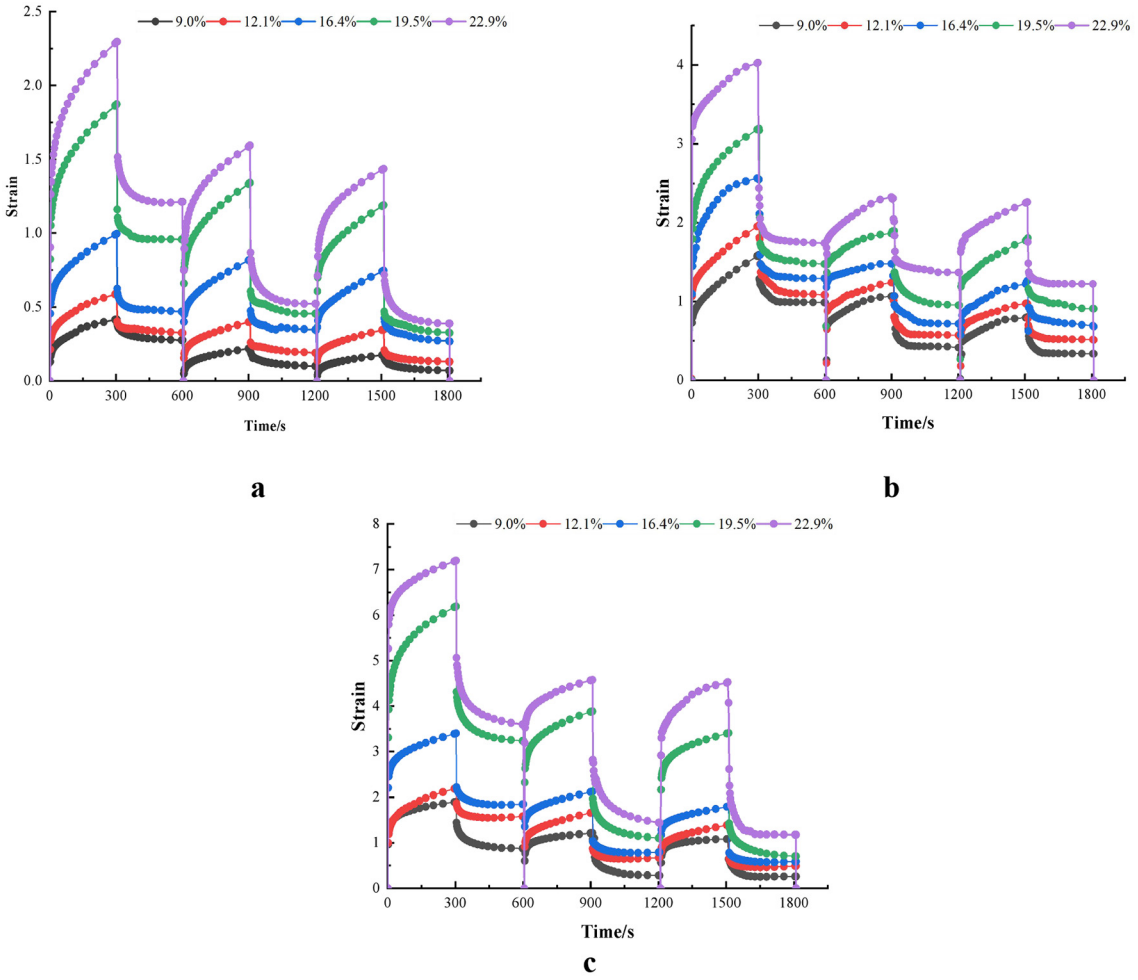

FIGURE 6
The creep curves of highland barley grains under different moisture contents. **(a)** Beiqing-7, **(b)** Kunlun-15, and **(c)** Yunqing-8 varieties. Stress = 0.02 MPa.

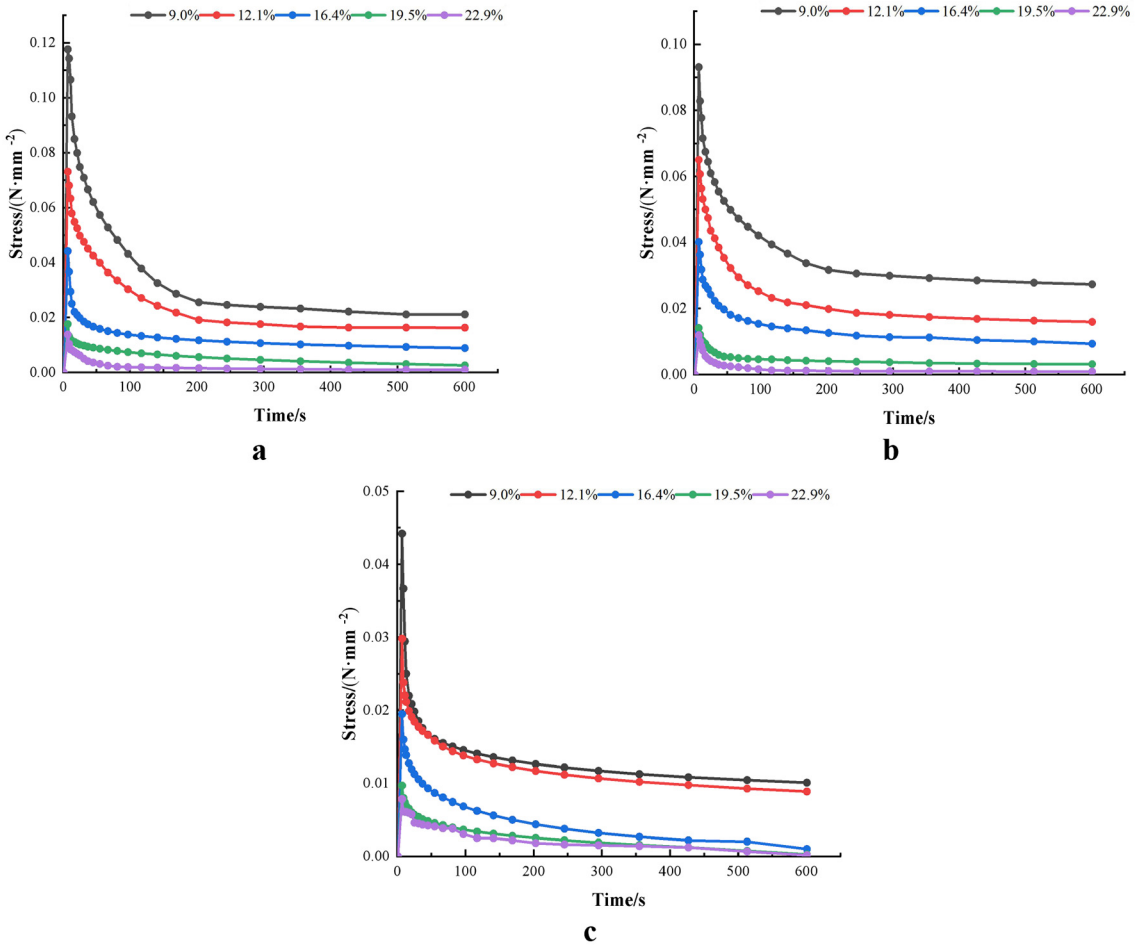

FIGURE 7
The stress relaxation curves of highland barley grains under different moisture contents. **(a)** Beiqing-7, **(b)** Kunlun-15, and **(c)** Yunqing-8 varieties. Strain = 0.8%.

decreased, indicating reduced elasticity and hardness of the grains. As the height of the creep curve increased, the viscosity coefficient η decreased, and the lag time τ_r showed a decreasing trend. Under the same moisture content, E_0, E_r, and η increased with cycle number, with the third cycle greater than the second and the second greater than the first, whereas τ_r showed no notable differences. These trends are consistent with those reported for maize kernels (Sheng, 2016) and highland barley grains (Zhu et al., 2017).

Under the same moisture content, the relaxation process includes two stages (Figure 7). The first stage is the elastic deformation of the highland barley sample after the load is applied for a short time. In the second stage, when the strain (0.8) was maintained, the stress in the highland barley grain samples gradually decreased. When the set strain was reached, the stress in the grain decreased with time and finally reached an equilibrium value. When the moisture content was between 9.0% and 22.9%, the stress of the grain simultaneously decreased with an increase in moisture content. The stress relaxation curves of the three varieties were similar, with Beiqing-7 used as an example. The three-element Maxwell model was used to fit the stress relaxation process of highland barley grains, and the regression models and significant P-values are listed in Table 9. The significant P-values of the regression models were less than 0.0001, indicating that the regression models fit the data well.

Table 9 shows that as the moisture content increased, the decay elastic modulus E_1 and equilibrium elastic modulus E_c of highland barley grains decreased, whereas the relaxation time τ_1 increased. Similar trends have been reported for maize kernels (Sheng, 2016).

4 Discussion

The physical parameters of highland barley grains are important in the design of highland barley harvesters, seeders, and other related machinery (Jin, 2024). The parameters of the different varieties under different moisture contents can be directly applied to the design and optimization of the corresponding machinery. If the moisture content corresponding to the required parameters is not within the experimental range of this study, the corresponding values can be calculated using an interpolation method to satisfy the requirements of practical engineering design.

TABLE 8 Regression models and significant *P*-values of the highland barley grain creep experiment results.

Moisture content/%	Creep model	Cycle period	Regression model	*P*-value
9.0	Burgers model	Cycle1	$\varepsilon(t)=\frac{\sigma}{0.141}+\frac{\sigma}{0.136}\left[1-e^{(-t/25.063)}\right]+\frac{\sigma}{42.778}t$	<0.0001
		Cycle2	$\varepsilon(t)=\frac{\sigma}{0.348}+\frac{\sigma}{0.237}\left[1-e^{(-t/22.1652)}\right]+\frac{\sigma}{70.411}t$	<0.0001
		Cycle3	$\varepsilon(t)=\frac{\sigma}{0.449}+\frac{\sigma}{0.228}\left[1-e^{(-t/23.642)}\right]+\frac{\sigma}{89.435}t$	<0.0001
12.1		Cycle1	$\varepsilon(t)=\frac{\sigma}{0.082}+\frac{\sigma}{0.115}\left[1-e^{(-t/23.574)}\right]+\frac{\sigma}{31.807}t$	<0.0001
		Cycle2	$\varepsilon(t)=\frac{\sigma}{0.120}+\frac{\sigma}{0.188}\left[1-e^{(-t/23.681)}\right]+\frac{\sigma}{43.519}t$	<0.0001
		Cycle3	$\varepsilon(t)=\frac{\sigma}{0.136}+\frac{\sigma}{0.225}\left[1-e^{(-t/25.247)}\right]+\frac{\sigma}{50.058}t$	<0.0001
16.4		Cycle1	$\varepsilon(t)=\frac{\sigma}{0.041}+\frac{\sigma}{0.084}\left[1-e^{(-t/22.355)}\right]+\frac{\sigma}{20.150}t$	<0.0001
		Cycle2	$\varepsilon(t)=\frac{\sigma}{0.047}+\frac{\sigma}{0.126}\left[1-e^{(-t/26.400)}\right]+\frac{\sigma}{23.198}t$	<0.0001
		Cycle3	$\varepsilon(t)=\frac{\sigma}{0.052}+\frac{\sigma}{0.147}\left[1-e^{(-t/28.755)}\right]+\frac{\sigma}{25.045}t$	<0.0001
19.5		Cycle1	$\varepsilon(t)=\frac{\sigma}{0.022}+\frac{\sigma}{0.040}\left[1-e^{(-t/14.331)}\right]+\frac{\sigma}{11.210}t$	<0.0001
		Cycle2	$\varepsilon(t)=\frac{\sigma}{0.028}+\frac{\sigma}{0.069}\left[1-e^{(-t/21.260)}\right]+\frac{\sigma}{15.920}t$	<0.0001
		Cycle3	$\varepsilon(t)=\frac{\sigma}{0.031}+\frac{\sigma}{0.085}\left[1-e^{(-t/20.467)}\right]+\frac{\sigma}{17.922}t$	<0.0001
22.9		Cycle1	$\varepsilon(t)=\frac{\sigma}{0.021}+\frac{\sigma}{0.026}\left[1-e^{(-t/10.375)}\right]+\frac{\sigma}{9.259}t$	<0.0001
		Cycle2	$\varepsilon(t)=\frac{\sigma}{0.026}+\frac{\sigma}{0.045}\left[1-e^{(-t/15.145)}\right]+\frac{\sigma}{14.823}t$	<0.0001
		Cycle3	$\varepsilon(t)=\frac{\sigma}{0.027}+\frac{\sigma}{0.052}\left[1-e^{(-t/14.340)}\right]+\frac{\sigma}{17.478}t$	<0.0001

TABLE 9 Regression models and significant *P*-values of the highland barley grain stress relaxation experiment results.

Moisture content/%	Relaxation model	Regression model	*P*-value
22.9	Three-element Maxwell model	$\sigma(t)=0.0314\cdot e^{(-t/12.886)}+0.0129$	<0.0001
19.5		$\sigma(t)=0.0152\cdot e^{(-t/33.824)}+0.0110$	<0.0001
16.4		$\sigma(t)=0.0138\cdot e^{(-t/52.856)}+0.00291$	<0.0001
12.1		$\sigma(t)=0.00668\cdot e^{(-t/64.606)}+0.00142$	<0.0001
9.0		$\sigma(t)=0.0057\cdot e^{(-t/73.194)}+0.00103$	<0.0001

Figure 6 shows that under the same moisture content, when the same load was applied, the strain of Yunqing-8 was the largest, and that of Beiqing-7 was the smallest. Figures 7a–c reveals that when the same strain was generated, the required stress of Beiqing-7 was the largest, and that of Yunqing-8 was the smallest. Combined with the analysis results of the physical and shear properties of different varieties, these findings show that the grains of Beiqing-7 are fuller and have better mechanical properties (Chen, 2025). Hence, in the breeding of highland barley varieties, the selection of varieties with better mechanical properties is conducive to reducing the damage rate of grains during harvesting, threshing, and other processes.

The internal and external friction characteristics of the grains are expressed by the friction coefficient and angle of repose, respectively. The angle of repose is an important parameter for calculating storage pressure (Yang et al., 2016). In addition to the moisture content, friction materials, and varieties, the friction coefficient may also be related to the size and arrangement of the grains. In addition to the moisture content and varieties, the angle of repose may also be related to the size, arrangement, and falling height of the grains. Therefore, future studies should aim to investigate the influence of these factors on the friction coefficient and angle of repose.

In this study, the effects of highland barley varieties and moisture content on the mechanical properties of highland barley grains were examined. A correlation exists between the shear force of wheat and its starch and protein content (Cheng and Sun, 2009). Therefore, in the future, the effects of starch and protein content on the shear mechanical properties of highland barley grains should be investigated.

5 Conclusion

In this study, by examining the effects of highland barley varieties and moisture content on the physical parameters, such as triaxial size and sphericity, and mechanical properties, such as shear, friction, angle of repose, and viscoelasticity, of highland barley grains, the following conclusions were drawn.

(1) The geometric dimensions (length, width, height, arithmetic mean diameter, geometric mean diameter, and sphericity) and 1,000-grain weight of highland barley grains increased substantially as the moisture content increased, whereas the unit weight decreased. This change was mainly caused by the expansion of the grains after water absorption. Differences among varieties were evident, and the overall indices of Beiqing-7 were the highest.

(2) The shear failure force and failure stress increased linearly with a decrease in moisture content, the deformation decreased gradually, and the failure energy initially decreased and subsequently increased non-linearly. Variety and moisture content were crucial influencing factors, with moisture content

being the main influencing factor. The shear mechanical indices of Beiqing-7 were generally the highest.

(3) The friction coefficient and angle of repose increased as the moisture content increased and were markedly affected by the surface roughness of the friction materials. The friction coefficient of the Q235 steel plate was the highest. The differences among varieties were consistent; the friction coefficient of Yunqing-8 was the largest, and the angle of repose of Beiqing-7 was the largest. Overall, moisture content was the most important factor affecting the friction characteristics.

(4) The creep behavior of grains under a constant load can be divided into three stages: instantaneous elasticity, delayed elasticity, and viscous flow. The Burgers model fit the data well ($R^2 > 0.99$). An increase in moisture content led to a decrease in the instantaneous elastic modulus and delayed elastic modulus and an increase in creep deformation, indicating that the elasticity and hardness of the grains decreased.

(5) The stress relaxation process can be described using a three-element Maxwell model ($R^2 > 0.98$). An increase in moisture content reduced the equilibrium elastic modulus and decay elastic modulus and prolonged the relaxation time. With an increase in the number of loading cycles at the same moisture content, the elastic modulus and viscosity coefficient increased, whereas the lag time did not change substantially.

The research results can provide a basis for the simulation and optimization design of highland barley harvesters, seeders, and related machinery.

Data availability statement

The raw data supporting the conclusions of this article will be made available by the authors, without undue reservation.

Author contributions

JS: Software, Data curation, Writing – original draft, Conceptualization, Writing – review & editing, Investigation, Funding acquisition. SQ: Funding acquisition, Writing – review & editing, Supervision, Methodology, Software. HF: Software, Methodology, Investigation, Supervision, Writing – review & editing. YG: Conceptualization, Methodology, Writing – review & editing. BX: Software, Writing – review & editing.

Funding

The author(s) declared that financial support was received for this work and/or its publication. This research was funded by the National Natural Science Foundation of China Youth Science Foundation Project (No. 52305268), Fundamental Research Program of Shanxi Province, China (Project No. 20210302124521), Yuncheng University Excellent Doctor to Shanxi Province Scientific Research Project (Project No. QZX-2020007), Yuncheng University Doctoral Research Start-up Program (Project No.: YQ-2023060), Yuncheng University 2025 Teaching Reform and Innovation Project (Project No. JG202539), Yuncheng University 2025 College Students' Innovative Training Program Project (Project No. 202510123005), and Yuncheng University Mechanical Engineering Discipline Funds.

Acknowledgments

The authors would like to thank the Department of Mechanical and Electrical Engineering at Yuncheng University and the College of Agricultural Engineering at Shanxi Agricultural University for providing the facilities and institutional support required to carry out this research. We also thank the researchers and collaborators who contributed to the development of this study.

Conflict of interest

The author(s) declared that this work was conducted in the absence of any commercial or financial relationships that could be construed as a potential conflict of interest.

Generative AI statement

The author(s) declared that generative AI was not used in the creation of this manuscript.

Any alternative text (alt text) provided alongside figures in this article has been generated by Frontiers with the support of artificial intelligence and reasonable efforts have been made to ensure accuracy, including review by the authors wherever possible. If you identify any issues, please contact us.

Publisher's note

References

Carvalho, G., Polachini, T., Augusto, P., Telis-Romero, J., and Bon, J. (2021). Physical properties of barley grains at hydration and drying conditions of malt production. *J. Fo. Pro. Eng.* 4:e13644. doi: 10.1111/jfpe.13644

Chen, J., Zhao, N., Fu, N., Li, D., Wang, L., and Chen, X. (2019). Mechanical properties of hulless barley stem with different moisture contents. *Int. J. Food Eng.* 15:20180033. doi: 10.1515/ijfe-2018-0033

Chen, L. (2025). *Research on the Crushing Characteristics and Crack Propagation Law of Wheat Grains*. Zhengzhou, China: Henan University of Technology.

Cheng, Y., and Sun, X. (2009). Relationships between anti-shearing force and quality properties of wheat grain. *Trans. Chi. Soc. Agr. Eng.* 25, 314–316. doi: 10.3969/j.issn.1002-6819.2009.06.059

Cui, Q., Hou, H., Zheng, D., and Wu, Z. (2016). Design and test of tilt dise-type fine and small-amount seed metering device for Foxtail Millet. *Trans. Chi. Soc. Agr. Eng*. 32, 17–23. doi: 10.11975/j.issn.1002-6819.2016.12.003

Dai, F., Zhang, S., Zhao, W., Shi, R., Tian, B., and Xin, S. (2021). Parameter optimization and experiment of highland barley combine harvester with baler. *Agr. Resh. Arid Areas*. 39, 248–256. doi: 10.7606/j.issn.1000-7601.2021.06.29

Ding, W. (2022). *Study on Reverse Rotary Tillage -Uniform Sowing Technology and Equipment of Highland Barley* (Thesis). Chinese Academy of Agricultural Sciences, Beijing, China.

Ding, W., Zhu, J., Chen, W., Zhang, J., Yuan, D., and Ding, Y. (2021). Simulation calibration of highland barley contact parameters based on EDEM. *J. Chi. Agr. Mech*. 42, 114–121. doi: 10.13733/j.jcam.issn.2095-5553.2021.09.16

Duan, Y., Cui, J., Xu, S., Wang, J., Liu, H., Yang, L., et al. (2023). Genome-wide association analysis and candidate gene mining for grain type-related traits in japonica rice. *Acta Agri. Boreali - Sin.* 38, 19–28. doi: 10.7668/hbnxb.20193821

He, X., Li, M., Wang, J., Wang, R., Zhang, S., Song, Y., et al. (2025). The effect of moisture content on physical properties and milling quality of wheat. *Sci. Tec. Fo. Ind*. doi: 10.13386/j.issn1002-0306.2025070385

Jia, H., Wu, W., Wang, X., and Li, R. (2025). Design and experiments of the electro-mechanical integrated measurement device for a grain friction coefficient. *Trans. Chi. Soc. Agr. Eng.* 41, 31–41. doi: 10.11975/j.issn.1002-6819.202410066

Jin, F. (2024). *Optimization and Experimental Research on Working Parameters of Highland Barley Harvesting Equipment Cleaning Device* (Thesis). Chinese Academy of Agricultural Sciences, Beijing, China.

Li, X., Cong, X., Yang, G., Li, F., Liang, L., and Quan, Z. (2022). Effects of different processing technologies of soybean meal on pellet feed processing characteristics, nutrient apparent digestibility and serum immune indices of meat rabbits. *Chin. J. Ani Agri. Nutri.* 34, 6677–6686. doi: 10.3969/j.issn.1006-267x.2022.10.060

Li, Y., Yin, Y., Xu, S., and Jin, W. (2025). *Physical Properties of Foods, 3rd Edn*. Beijing: China Light Industry Press, 77–100.

Liang, L., Wang, S., Jia, J., and Feng, Z. (2022). Relationship between grain quality traits and fermentation quality of xiaoqu liquor from different hulless barley cultivars. *Food Sci.* 43, 27–32. doi: 10.7506/spkx1002-6630-20220110-076

Liu, K. (2020). *Experimental Study on Cleaning Characteristics of Harvested Barley by Machinery*. Taigu, China: Shanxi Agricultural University.

Liu, Y. (2023). *Simulation of Hot Air Drying Characteristics and Heat Mass Transfer in High Moisture Wheat*. Zhengzhou, China: Henan University of Technology.

Lu, C. (2024). *Design and Experiment of a Hand-Pushed Multifunctional Vegetable Seeder*. Chongqing, China: Chongqing Three Gorges University.

Ma, Y. (2015). *Agricultural Materials Science.* Beijing: Chemical Industry Press, 21–47.

Ouyang, A., Wang, M., Cui, T., and Wang, C. (2024). Application status and development trend of mechanized equipment for grain crop production. *J. Chin. Agri. Mech.* 45, 298–304. doi: 10.13733/j.jcam.issn.2095-5553.2024.10.043

Qiu, S., Li, L., Cui, Q., Yang, Z., Feng, Y., and Guo, Y. (2021). Research of shearing characteristics of bare oat grain. *J. Chi. Agr. Mech*. 42, 67–71. doi: 10.13733/j.jcam.issn.2095-5553.2021.06.11

Qiu, S., Yuan, X., Guo, Y., Cui, Q., Wu, X., and Zhang, Z. (2019). Effects of variety and moisture content on mechanical properties of millet. *Trans. Chi. Soc. Agr. Eng*. 35, 322–326. doi: 10.11975/j.issn.1002-6819.2019.24.038

Sheng, S. (2016). *Study on Drying Characteristics and Viscoelastic Behaviors of Maize Kernels*. Beijing, China: China Agricultural University.

Sologubik, C., CampañoneA, L., Pagano, A., and Gely, M. (2013). Effect of moisture content on some physical properties of barley. *Ind. Crops Prod*. 43, 762–767. doi: 10.1016/j.indcrop.2012.08.019

Song, Y. (2019). *Highland Barley Seeds processing: Germination for Selenium Enrichment, Ultrasound Enhanced Hot Air Drying for Dehydration and Beverage*. Nanjing, China: Nanjing Agricultural University.

Sun, F., Zhang, T., Dai, C., He, C., Ciren, D., Shi, J., et al. (2024). Determination and contamination of mycotoxins in highland barley grain samples from Xizang. *J. Chi Cereals Oils Assoc*. 39, 189–195. doi: 10.20048/j.cnki.issn.1003-0174.000730

Sun, J., Guo, Y., Yang, Z., Cui, Q., Wu, X., and Zhang, Y. (2018). Experimental study on biomechanical properties of buckwheat grain and viscoelastic properties of buckwheat powder. *Trans. Chi. Soc. Agr. Eng.* 34, 287–298. doi: 10.11975/j.issn.1002-6819.2018.23.037

Wang, B. (2023). *Design and Research on Harvest Cutting Table and The Mechanical Properties of Highland Barley Stem*. Lanzhou, China: Science Horticulture Gansu Agricultural University.

Wang, X., Bai, Y., Yao, X., Yao, Y., Li, X., An, L., et al. (2023). Effect of mowing stubble height on forage and grain yield and forage quality characteristics of hulless barley. *J. Triticeae Crops*. 43, 513–523. doi: 10.7606/j.issn.1009-1041.2023.04.14

Wei, L. (2016). *The Design of Plot Wheat Breeding Threshing Machine and Research on It's Low Damage Characteristics*. Lanzhou, China: Gansu Agricultural University.

Yang, Z., Guo, Y., Cui, Q., and Li, H. (2016). Test and influence factors analysis of friction characteristics of millet. *Trans. Chi. Soc. Agr. Eng.* 32, 258–264. doi: 10.11975/j.issn.1002-6819.2016.16.035

Yang, Z., Sun, J., and Guo, Y. (2015). Effect of moisture content on compression mechanical properties and frictional characteristics of millet grain. *Trans. Chi. Soc. Agr. Eng.* 31, 253–260. doi: 10.11975/j.issn.1002-6819.2015.23.034

Zha, S., and Wang, M. (2023). Lipid metabolomics of different highland barley cultivars during storage. *J. Chi Cereals Oils Assoc.* 38, 110–116. doi: 10.20048/j.cnki.issn.1003-0174.000191

Zhang, X., Han, M., Li, Y., Liu, M., Zhou, X., Li, Y., et al. (2025). The differences in nutritional quality and antioxidant capacity of colored highland barley. *J. Chi Cereals and Oils Association*. 40, 80–87. doi: 10.20048/j.cnki.issn.1003-0174.001155

Zhu, K., Zhao, R., and Xing, J. (2023). *Principles of Grain Science, 2nd Edn*. Beijing: China Light Industry Press, 137–149.

Zhu, X., Chi, R., and Ma, Y. (2023). Effects of corn varieties and moisture content on mechanical properties of corn. *Agronomy* 13:545. doi: 10.3390/agronomy13020545

Zhu, Y., Fu, N., Li, D., Wang, L., and Chen, X. (2017). Physical and viscoelastic properties of different moisture content highland barley kernels. *Int. J. Fo Eng.* 13:20170186. doi: 10.1515/ijfe-2017-0186